LEVEL II

COMPRESSIVE STRENGTH AND DAMAGE MECHANISMS IN CERAMIC MATERIALS

I. The Role of Subcritical Tensile Microfracture
   Processes in Compression Failure of Ceramics
II. Electron Channeling Study of Fracture
   in Alumina — Evidence for Crack Tip Plasticity

by

James Lankford
David L. Davidson

INTERIM TECHNICAL REPORT

For

Office of Naval Research
Arlington, Va 22217

Prepared by
Southwest Research Institute
San Antonio, Texas

September 1981

DTIC
ELECTE
NOV 17 1981
E

AD A107 61

DTIC FILE COPY

SOUTHWEST RESEARCH INSTITUTE
SAN ANTONIO   HOUSTON

REPORT DOCUMENTATION PAGE		READ INSTRUCTIONS BEFORE COMPLETING FORM
1. REPORT NUMBER	2. GOVT ACCESSION NO. AD-A107617	3. RECIPIENT'S CATALOG NUMBER
4. TITLE (and Subtitle) Compressive Strength and Damage Mechanisms in Ceramic Materials		5. TYPE OF REPORT & PERIOD COVERED Interim Technical Report 1 Sept. 1980 - 30 Sept. 1981
		6. PERFORMING ORG. REPORT NUMBER 02-4231
7. AUTHOR(s) James Lankford David L. Davidson		8. CONTRACT OR GRANT NUMBER(s) N00014-75-C-0668
9. PERFORMING ORGANIZATION NAME AND ADDRESS Southwest Research Institute 6220 Culebra Road (P. O. Drawer 28510) San Antonio, TX 78284		10. PROGRAM ELEMENT, PROJECT, TASK AREA & WORK UNIT NUMBERS NR 032-553/1-3-75(471)
11. CONTROLLING OFFICE NAME AND ADDRESS Office of Naval Research 800 North Quincy Arlington, VA 22217		12. REPORT DATE September 1981
		13. NUMBER OF PAGES 31 + prelims.
14. MONITORING AGENCY NAME & ADDRESS(if different from Controlling Office)		15. SECURITY CLASS. (of this report) UNCLASSIFIED
		15a. DECLASSIFICATION/DOWNGRADING SCHEDULE

16. DISTRIBUTION STATEMENT (of this Report)

approved
and sale; its
limited.

17. DISTRIBUTION STATEMENT (of the abstract entered in Block 20, if different from Report)

18. SUPPLEMENTARY NOTES

19. KEY WORDS (Continue on reverse side if necessary and identify by block number)

Compressive Strength	Crack Tip Plasticity	Cavitation
Silicon Carbide	Temperature Effects	Fracture Mechanisms
Silicon Nitride	Strain Rate Effects	Ceramics
Aluminum Oxide	Tensile Microfracture	

20. ABSTRACT (Continue on reverse side if necessary and identify by block number)

The compressive strength of SiC, Si_3N_4, and Al_2O_3 is investigated over wide ranges in temperature and loading rate. Several distinct damage regimes are identified, all based upon tensile microfracture processes. Two aspects of the work are of special interest. The first is the identification of a high strain rate regime in which material inertial effects are responsible for unusually rapid strengthening; the basis for the effect is increased difficulty in either crack nucleation or extension. Secondly, it is found that at low loading rates, subcritical tensile microcrack growth is responsible for a

DD FORM 1 JAN 73 1473

thermally activated strength dependence. Selected area electron channeling experiments lead to the conclusion that the thermal activation process may involve crack tip plasticity.

TABLE OF CONTENTS

LIST OF ILLUSTRATIONS

I

THE ROLE OF SUBCRITICAL TENSILE MICROFRACTURE PROCESSES IN COMPRESSION FAILURE OF CERAMICS

James Lankford

Department of Materials Sciences
Southwest Research Institute
San Antonio, Texas 78284 USA

ABSTRACT

The compressive strengths of several engineering ceramics (Al_2O_3, α-SiC, NC 132, NC 350) have been determined over a wide range in strain rate. From very low strain rates, to rates on the order of $10^2 sec^{-1}$, the strength for each material increased according to a relationship which correlated with K-V fracture mechanics data, suggesting that in this regime, compression failure was actually governed by thermally activated growth of axially-oriented Mode I (tensile) microcracks. At strain rates above $10^2 sec^{-1}$ (achieved through Hopkinson pressure bar tests), a sudden increase in the rate of strengthening with deformation rate was observed for all of the materials except the NC 350. This increase was interpreted in terms of inertia-controlled (i.e., non-thermally activated) growth of axial, Mode I microcracks. For NC 350, an unexpected decrease in strength was observed at strain rates on the order of $10^3 sec^{-1}$. This effect was found to correspond to a change in failure mode from transgranular to intergranular fracture; for the other materials, failure was transgranular at all strain rates. Implications of the results with regard to microfracture during rapid impact by sharp hard particles are discussed.

INTRODUCTION

There is considerable current interest in the problem of microfracture during the impact of strong ceramics by small hard particles. It is known that the subsurface zone beneath a particle impact site is subjected to immense transient compressive

loads, sufficient to cause plastic flow and to nucleate cracks.[1] In order to gain further insight into the latter process, dynamic compression experiments have been carried out for a variety of ceramics over a strain rate range of nearly eight orders of magnitude.

EXPERIMENTAL APPROACH

Experimental details are given in detail elsewhere,[2,3] and hence are outlined only briefly here. Materials studied included Lucalox alumina,[*] sintered α-SiC,[**] hot-pressed silicon nitride[+] (NC 132), and reaction-bonded silicon nitride[+] (NC 350). Cylindrical specimens of each material were ground and polished,[2] and compressed at 23°C using platens of α-SiC for the SiC specimens, and high strength, high purity alumina for the other materials. Low speed tests were performed in a servo-controlled hydraulic machine, yielding strain rates of $7 \times 10^{-5} \text{sec}^{-1}$ and $2 \times 10^{-1} \text{sec}^{-1}$. High strain rates, on the order of 10^3sec^{-1}, were achieved by use of a Hopkinson pressure bar. It is estimated[4] that the latter rate would correspond to an impact velocity of 10-100 m/sec. Broken specimens were studied fractographically within the SEM.

RESULTS

Results of the strength tests are shown in Figure 1, in which compressive strength σ_c is plotted versus strain rate $\dot{\epsilon}$ for all four materials. Included is a Lucalox data point (the average of several tests) at a strain rate of $\dot{\epsilon} \sim 10^4 \text{sec}^{-1}$, obtained by Munson and Lawrence[5] using a Hugoniot shock technique. For $\dot{\epsilon} < 10^0 \text{sec}^{-1}$, strength increases gradually with strain rate for Al_2O_3 and NC 350, and is essentially constant for SiC and NC 132. Above $\dot{\epsilon} \sim 10^0 \text{sec}^{-1}$, the strength of the NC 350 decreases, while for the other materials, the low strain rate trend transits at $\dot{\epsilon} \sim 10^3 \text{sec}^{-1}$ to a regime in which the strength begins to increase very rapidly with $\dot{\epsilon}$.

It is interesting to note that weaker "ceramics" can behave in a similar fashion, as shown in Figure 2. Data[6] for fine-grained, competent (low porosity) Solenhofen limestone, whose average strength is lower by an order of magnitude than that of the four ceramics, show the same pattern of a very gradual strength increase with strain rate until $\dot{\epsilon} \sim 10^3 \text{sec}^{-1}$, where upon the

---

[*]G.E. Lamp Glass Division, Cleveland, Ohio
[**]Carborundum Corporation, Niagara Falls
[+]Norton Company
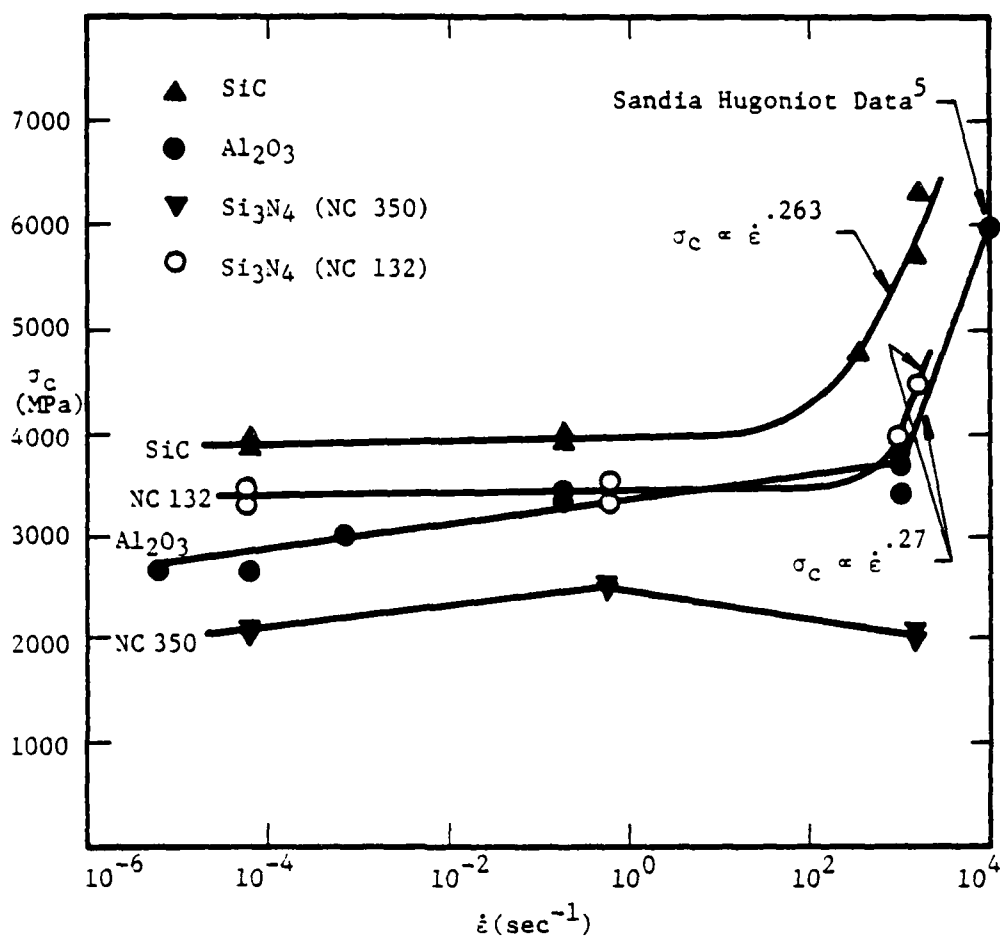
Fig. 1. Compressive strength versus strain rate.

strength dependence becomes much more sensitive. For both the ceramics and the limestone, the slope of the σ_c-$\dot{\epsilon}$ curve in the latter region is essentially identical, i.e., ~0.3.

Fractographic analysis showed that most of the ceramics failed in a transgranular mode over the entire compressive strain rate range (Figures 3-5). On the other hand, while NC 350 also failed transgranularly for $\dot{\epsilon} \stackrel{<}{\sim} 2 \times 10^{-1} \text{sec}^{-1}$ (Figure 6a), its fractography was clearly intergranular at $\dot{\epsilon} = 2 \times 10^{3} \text{sec}^{-1}$ (Figure 6b).
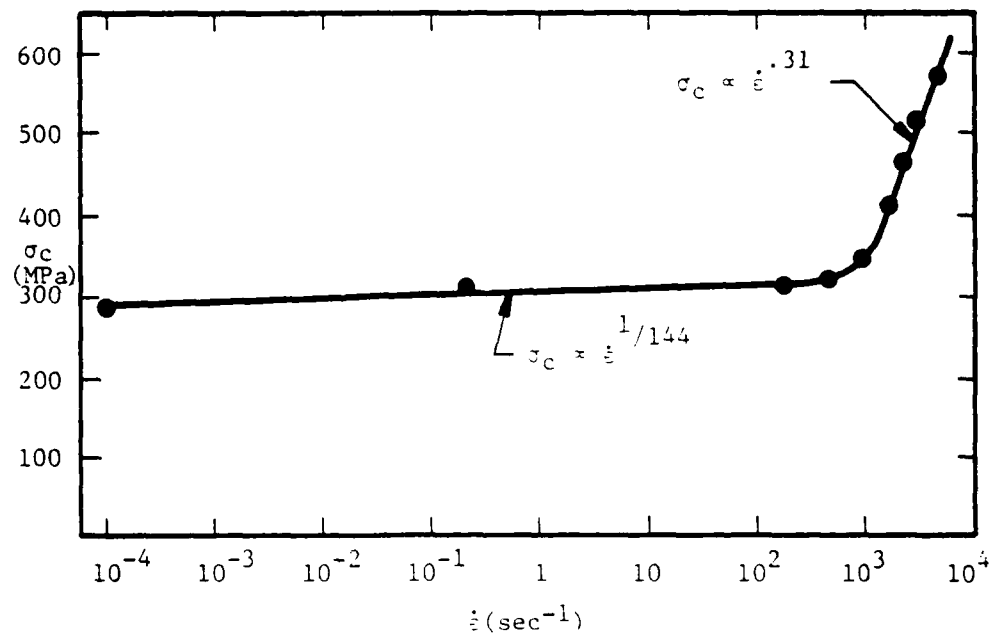
Fig. 2. Compressive strength versus strain rate for Solenhofen limestone.[6]

Fig. 3. Al_2O_3 transgranular fracture, all $\dot{\varepsilon}$.

Fig. 4. α-SiC transgranular fracture, all ε̇.

Fig. 5. NC 132 transgranular fracture, all ε̇.

(a) Transgranular fracture, $\dot{\varepsilon} = 7 \times 10^{-5} s^{-1}$ and $2 \times 10^{-1} s^{-1}$.

(b) Intergranular fracture, $\dot{\varepsilon} = 2 \times 10^{3} s^{-1}$.

Fig. 6. NC 350 fractography.

DISCUSSION

In the low strain rate regime ($\dot{\varepsilon} \lesssim 10^2 \text{sec}^{-1}$), it is possible to describe the results* in terms of
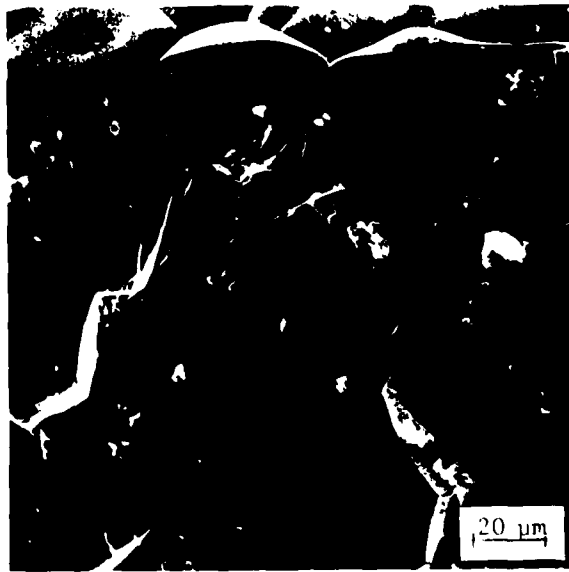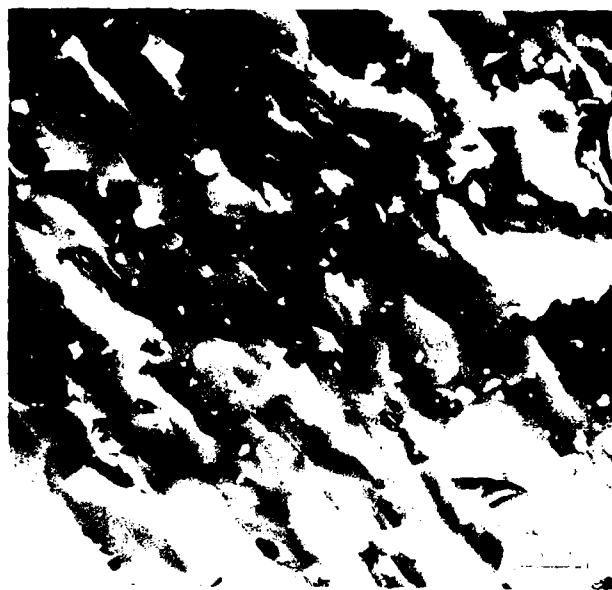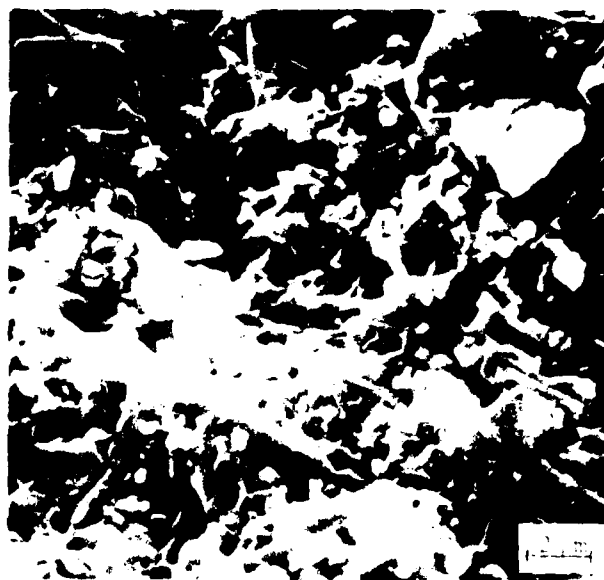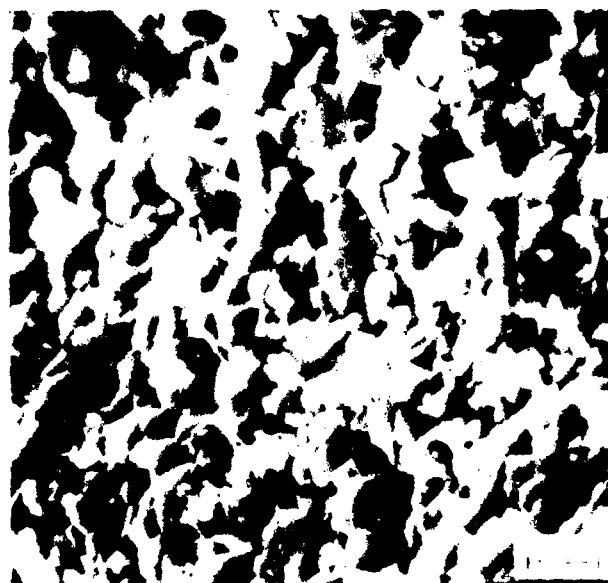
$$\sigma_c \propto \dot{\varepsilon}^{1/1+n_c} \tag{1}$$

analogous to the relation

$$\sigma_T \propto \dot{\varepsilon}^{1/1+n_T} \tag{2}$$

which has been shown[7] to correlate tensile strength σ_T with $\dot{\varepsilon}$; n_c and n_T are constants. Experiments have shown that $n_T \approx n$, the exponent in the fracture mechanics relationship[11]

$$V = AK^n \tag{3}$$

where V is the growth velocity of a Mode I tensile crack in a fracture mechanics-type specimen subject to a stress intensity K, and A is a constant. This observed equivalence between n_T and n has been accepted as proof that the tensile strength-strain rate dependence is based on thermally activated, tensile microcrack growth.

Analysis of the data of Figures 1 and 2 according to Equation 1 yields the n_c values given in Table 1. The good agreement between n_c and n,** and the observed transgranular fracture modes for the four strong ceramics, suggest that for $\dot{\varepsilon} \lesssim 10^2 \text{sec}^{-1}$,

$$\sigma_c \propto \dot{\varepsilon}^{1/1+n} \tag{4}$$

and further, that this dependence arises from thermally activated, Mode I transgranular microcrack growth.

Earlier scanning electron microscopy work by the author has shown that the coalescence of axially oriented microcracks, nucleated by twins and sharp-edged grain boundary voids, is responsible for compressive failure in Al_2O_3[2] and α-SiC,[12] respectively.

Mechanisms by which tensile stresses acting across the face of axial cracks are produced within nominally compressive stress fields have been discussed by Tapponier and Brace[13]. For example,

---

*Ignoring momentarily the NC 350 dropoff in strength for $\dot{\varepsilon} \gtrsim 10^0 \text{sec}^{-1}$.
**From the work of other investigators, as referenced.

Table 1. Comparison of Compressive Strength-Strain Rate and Crack
Velocity-Stress Intensity Exponents ($\dot{\varepsilon} < 10^2 \text{sec}^{-1}$)

Material	n(K-V)	n_c (Compression)
Al_2O_3	52[8]	51
NC 350	57[9]	52
NC 132	very large[9]	very large
SiC	very large[10]	very large
Limestone	130[11]	143[6]

in Figure 7, a crack has nucleated at the grain boundary between
grains 1 and 2, forming an axial microcrack in grain 2. If the
grains are misoriented, so that their effective moduli (E') mis-
match across the boundary in such a way that the upper grain is
compliant relative to the stiffer lower grain, then a local ten-
sile stress will exist at the interface. This stress will be
proportional to $\nu(\frac{1}{E_1'} - \frac{1}{E_2'})$[14], where ν is Poisson's ratio.

Radial tension will therefore occur on the stiff side, reaching
significant fractions of the applied compressive stress for only
small differences in ν/E' between the two grains.[13]

The nature of the thermally activated process responsible for
the observed strain rate dependence via tensile crack growth is
not known with certainty, although there are (at least) several
possible explanations,[15] i.e., crack tip plasticity, stress-induced
vacancy diffusion, atomic bond fluctuation, or chemical processes
involving bond rearrangement. In support of the latter possibili-
ties, TEM experiments[15] have indicated the absence of crack tip
dislocations at indentation cracks in sapphire. On the other hand,
recent experiments by Lankford and Davidson[16] have revealed the
presence of damage (distortion) in electron channeling patterns
obtained from transgranular tensile fracture surfaces of Lucalox,
while channeling patterns of regions remote from the fracture re-
main undistorted. Currently, the only explanation for these
findings is the presence of near-surface dislocations associated
with passage of the crack.

It remains to consider the σ_c-$\dot{\varepsilon}$ regime of high strain rate
sensitivity. For $\dot{\varepsilon} > 10^2 \text{sec}^{-1}$,

$$\sigma_c \propto \dot{\varepsilon}^{.3} \qquad (5)$$

This relationship is relatively independent of material, with the
strain rate exponent varying from 0.263 to 0.31; similarly, the

σ

Grain 1
Compliant
$E_1{}'$

Grain 2
Stiff
$E_2{}' > E_1{}'$

σ
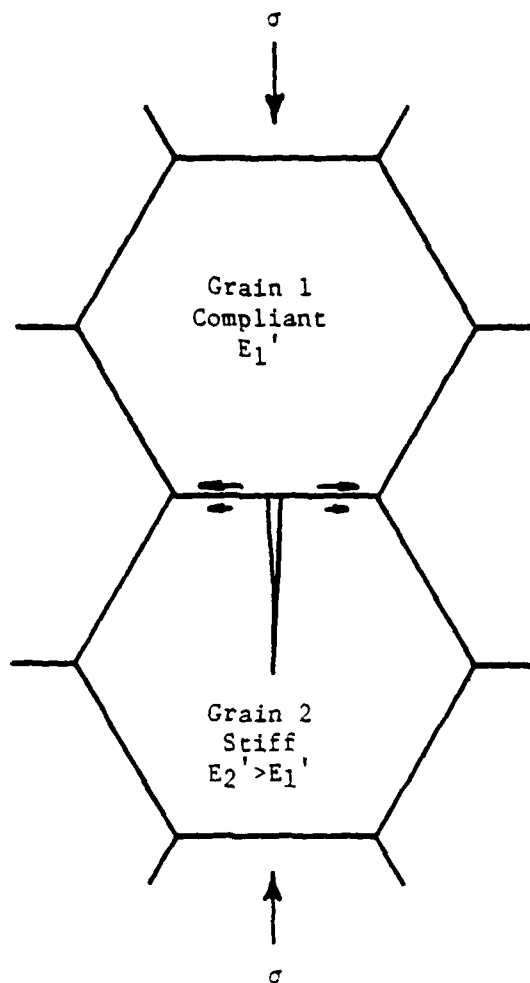
Fig. 7. Conceptual sketch of resolution of applied compressive
stress into local tensile stress normal to plane of axial
microcrack. Interfacial arrows represent unequal elastic
lateral displacements in the two grains, producing local
tensile stress field at the interface.[13]

transition from subcritical crack growth regime occurs, for all
four materials (neglecting the NC 350) between 10^3 and $10^4 sec^{-1}$.

It should first be noted that this effect cannot be construed
as an experimental, i.e., Hopkinson pressure bar (HPB), artifact.
For NC 350, the HPB data actually decrease, relative to the low $\dot{\epsilon}$
trend, and the transition to Equation 5 does not occur for Al_2O_3

until the HPB strain rate is exceeded. In fact, the relative constancy of the exponent is quite remarkable, considering that the date reflect three different sets of experiments (two HPB, one Hugoniot).

Actually, the observed high strain rate compression strengthening already has been predicted indirectly. Grady and his colleagues[17],[18] have considered the dynamic tensile failure of brittle materials, and allowing for the resolution of applied compressive stresses into local tensile microstresses as discussed above, one can make the following argument (after Grady and Kipp[17]). For quasi-static loading, the stress intensity of a penny-shaped crack of radius r_o subject to a tensile stress σ is given by

$$K_I = \frac{2}{\sqrt{\pi}} \sigma \sqrt{r_o} \tag{6}$$

However, for early times ($t < r_o/c$) during dynamic loading, the crack response exhibits a complex time dependence due to material inertia near the crack tip, whereby

$$K_I \approx \sigma \sqrt{ct} \tag{7}$$

where c is the speed of sound in the material. At failure, $K_I = K_{Ic}$, the fracture toughness, in which case the dynamic fracture stress is

$$\sigma_f \approx \frac{K_{Ic}}{\sqrt{ct_f}} \tag{8}$$

where t_f is the time to fracture initiation. Now, the strain rate to fracture can be written

$$\dot{\varepsilon} = \frac{\dot{\sigma}_f}{E} = \frac{\sigma_f}{\rho_o c^2 t_f} \tag{9}$$

where ρ_o is the material density. Eliminating t_f between Equations 8 and 9 yields the strain rate dependent fracture criterion

$$\sigma_f = \sqrt[3]{\rho_o c K_{Ic}^2} \; \dot{\varepsilon}^{1/3} \tag{10}$$

Hence

$$\sigma_f \propto \dot{\varepsilon}^{.33} \tag{11}$$

approximately as observed experimentally for high strain rates.

The lower bound strain rate $\dot{\varepsilon}^*$ for this regime should correspond to $ct_f = r_o$ = initial maximum flaw size. In this case

$$\sigma_f \sim \frac{K_{Ic}}{\sqrt{r_o}} \tag{12}$$

hence

$$\dot{\varepsilon}^* = K_{Ic}/\rho c r_o^{3/2} \tag{13}$$

For the ceramics (and rock) in this study,

$$10^3 < \dot{\varepsilon}^* < 10^4 \text{sec}^{-1} \tag{14}$$

over a wide (assumed) initial flaw size range (10-500 μm). This predicted strain rate range for the transition from subcritical crack growth, to material inertia, controlled fracture likewise agrees well with that observed in the experiments.

This scenario is summarized in Figure 8.[18] Under static loading ($\dot{\varepsilon}$-0), the largest existing crack will dominate. Under dynamic loading, however, cracks with a wide range in size are activated simultaneously, since their tips no longer have time to communicate. The higher the strain rate, the wider the size range of activated cracks.

The results of the high $\dot{\varepsilon}$ compressive strength tests for NC 350 cannot be explained at present. A possible (speculative) rationale is that the change in failure mode from transgranular to intergranular is brought about through a grain boundary phase *transformation* induced by the high transient stresses produced during dynamic loading. The brittleness of this new grain boundary constituent could alter the failure process to the extent that the strength is lowered, and the transition to inertia-controlled failure shifted to a higher strain rate. Determination as to the validity of this suggestion will require further micro-structural characterization of NC 350, and compression tests at loading rate in excess of HPB capabilities.

CONCLUSIONS

Compressive failure in ceramics involves the nucleation and growth of axial microcracks within localized resolved tensile stress fields. For $\dot{\varepsilon} < 10^2 \text{sec}^{-1}$, $\sigma_c \propto \dot{\varepsilon}^{1/1+n}$, where n can be derived from K-V fracture mechanics tests. For $\dot{\varepsilon} > 10^2 \text{sec}^{-1}$, strength is inertia-controlled, and $\sigma_c \propto \dot{\varepsilon}^{0.3}$. At high loading rates, material inertia can produce very large strengthening effects, to the extent that for $\dot{\varepsilon} > 10^6 \text{sec}^{-1}$, the compressive
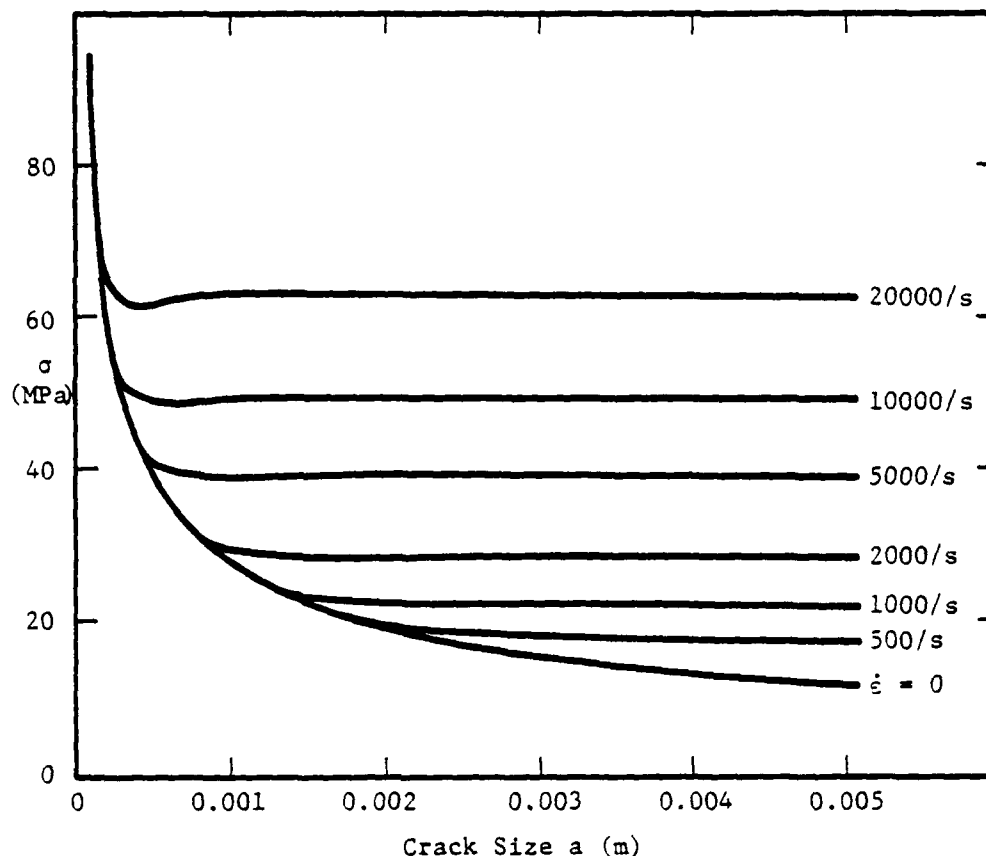
Fig. 8. Fracture stress for a penny-shaped crack under constant strain rate loading (typical rock).[18]

strength will approach the theoretical limit of $E/10$. Under such conditions, microcrack nucleation at correspondingly high particle impact velocities would be expected to be difficult.

REFERENCES

1. B. R. Lawn and M. V. Swain, J. Mat. Sci., 10 (1975) 113.
2. J. Lankford, J. Mat. Sci., 12 (1977) 791.
3. J. Lankford, Frac. Mech. Cer., Vol. 3, ed. R. C. Bradt,
      D. P. H. Hasselman, and F. F. Lange, Plenum Press, N.Y.
      (1978) 245.
4. A. G. Evans and T. R. Wilshaw, J. Mat. Sci., 12 (1977) 97.
5. D. E. Munson and R. J. Lawrence, J. Appl. Phys. 10 (1979)
      6272.
6. S. J. Green and R. D. Perkins, Proc. 10th Sym. Rock Mech.,
      ed. K. E. Gray (1968) 35.
7. A. G. Evans, Int. J. Frac., 10 (1974) 251.
8. A. G. Evans, M. Linzer, and L. R. Russell, Mat. Sci. Eng.,
      15 (1974) 253.
9. K. D. McHenry, T. Yonushonis, and R. E. Tressler, J. Am.
      Cer. Soc., 59 (1976) 262.
10. K. D. McHenry and R. E. Tressler, J. Am. Cer. Soc., 63
      (1980) 152.
11. J. P. Henry, J. Paquet, and J. P. Tancrez, Int. J. Rock
      Mech. Min. Sci. & Geomech. Abstr., 14 (1977) 85.
12. J. Lankford, J. Am. Cer. Soc., 62 (1979) 310.
13. P. Tapponier and W. F. Brace, Int. J. Rock Mech. Min. Sci. &
      Geomech. Abstr., 13 (1976) 103.
14. B. T. Prady, Int. J. Rock Mech. Min. Sci. & Geomech. Abstr.,
      8 (1971) 357.
15. S. M. Wiederhorn, B. J. Hockey, and D. E. Roberts, Phil.
      Mag., 28 (1973) 783.
16. J. Lankford and D. L. Davidson, J. Mat. Sci. (submitted).
17. D. E. Grady and M. E. Kipp, Int. J. Rock Mech. Min. Sci. &
      Geomech. Abstr., 16 (1979) 293.
18. M. E. Kipp, D. E. Grady, and E. P. Chen, Int. J. Frac., 16
      (1980) 471.

II

ELECTRON CHANNELING STUDY OF FRACTURE IN ALUMINA-EVIDENCE FOR CRACK TIP PLASTICITY

James Lankford and David L. Davidson

Department of Materials Sciences
Southwest Research Institute
San Antonio, Texas 78284, USA

ABSTRACT

The fracture surfaces of aluminum oxide specimens broken in bending are examined using selected area electron channeling. The distorted electron channeling patterns which result are interpreted as possible evidence of crack tip plasticity. The relationship of these findings to earlier experiments is discussed.

1.   Background

Whether or not plastic flow is associated with the fracture of aluminum oxide at low homologous temperatures ($\stackrel{\sim}{<}$ 900 C) has been a subject of investigation for several decades. Arguments for and against plasticity-controlled fracture of sapphire are summarized by Congleton, Petch, and Shiels [1], and by Wiederhorn, Hockey, and Roberts [2], respectively. The subject is important, because it relates to the physical basis of what seemingly should be, but is not [1], an athermal, Griffith-type process, controlled solely by surface free energy.

Studies to date have usually relied upon one or more of three experimental approaches: (1) transmission electron microscopy [2]; (2) X-ray diffraction [3]; (3) (interpretation of) mechanical tests in which temperature, stress rate, etc., are varied [1]. In the present paper, application to the problem of a relatively new technique, selected area electron channeling, is described. The results, although appearing to support the concept of crack tip plasticity during "brittle" fracture of alumina, are not conclusive in themselves. Consideration of the evidence gathered to date, both pro and con, suggests experimental approaches which might resolve the issue.

2.   Experimental Approach

Three-point bend tests were carried out under ambient conditions for two variations of as-fired Lucalox* rod. One set of specimens,

---

*G.E. Lamp Glass Division, Cleveland, Ohio.

broken during a fracture mirror/fractographic study by H. Kirshner, was characterized by a grain size of 15-20 μm. The other set was typical of material used in earlier tensile [4] and compressive [5] strength studies in this laboratory, and had a grain size of 24-40 μm. The fractured specimens were coated with a very thin layer of carbon, in order to permit conductivity within the SEM. This is a delicate process, since the coating must not be so thick as to destroy, through absorbtion, the diffraction contrast characteristic of backscattered electrons.

Electron channeling patterns were obtained by operating the SEM in the channeling mode, i.e., basically by rocking the beam about a stationary point within each grain of interest.[*] For grains in metals [7] and ceramics [6] which are free of plastic deformation, this process generates sharp, fine-structured electron channeling patterns; the presence of dislocation damage causes loss of higher order lines, broadening of other lines, and for sufficiently large deformation, the loss of contrast altogether. The spatial sensitivity (beam spot size) is probably 10-15 μm, the effective depth from which channeling information is obtained could extend to as much as 8 μm beneath the surface [8], and in metals, the technique is sensitive to plastic strains on the order of 0.003 [9].

---

[*]The channeling techinque is described in detail elsewhere [6].

3.   Results

This section will emphasize the results of electron channeling experiments carried out on the large-grained material, since no channeling contrast could be obtained from the fracture surfaces of the fine-grained alumina. Inspection of the outer surfaces of these specimens (Figure 1) showed evidence of extrusion. This process appears to have damaged the material to the extent that reference electron channeling patterns obtained from the outer surface were severely distorted.

On the other hand, Figure 2 shows a typical channeling pattern obtained from one of the nominally undeformed crystallities comprising the as-fired outer surface (Figure 3) of a large-grained specimen. All of the numerous outer grains which were investigated yielded patterns of similar quality, i.e., rich in fine structure and higher order re-flections, but slightly hazy due to the presence of the thin carbon deposit. We have obtained similar, but more sharply detailed, results for unde-formed SiC [10] which, being a semi-conductor, does not require a conductive surface coating.

An example of a typical Lucalox fracture surface is shown in Figure 4, where the apparent origin is near grain 1 (arrow). Numbers within grains correspond to channeling patterns in Figure 5, while dots denote grains in which efforts to obtain channeling patterns failed, i.e., the patterns (not shown in Figure 5) were a uniform gray tone, too diffuse to produce discernible line contrast.
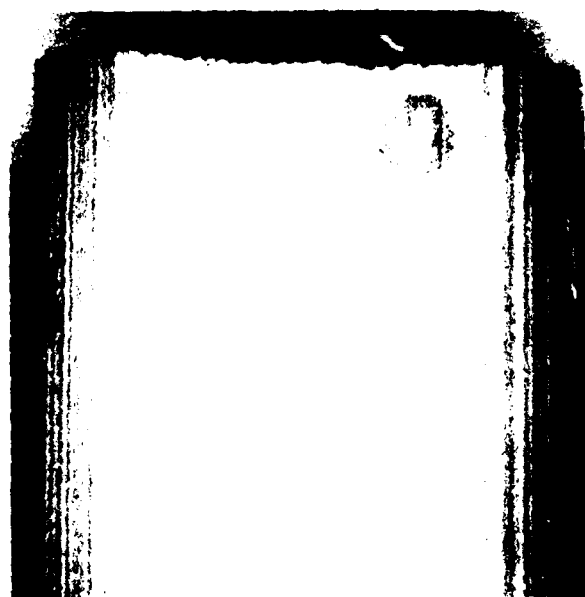
Figure 1.   Outer surface of fine-grained Lucalox bend specimen,
showing evidence of extrusion.   (12X)

Figure 2. Typical electron channeling pattern from (outer) surface grain of large-grained Lucalox specimen.

Figure 3. Outer surface of large-grained Lucalox bend specimen;
as-fired grains are visible. (12X)

Figure 4. Fracture surface of specimen broken in bending. Dots denote grains in which channeling patterns could not be obtained.
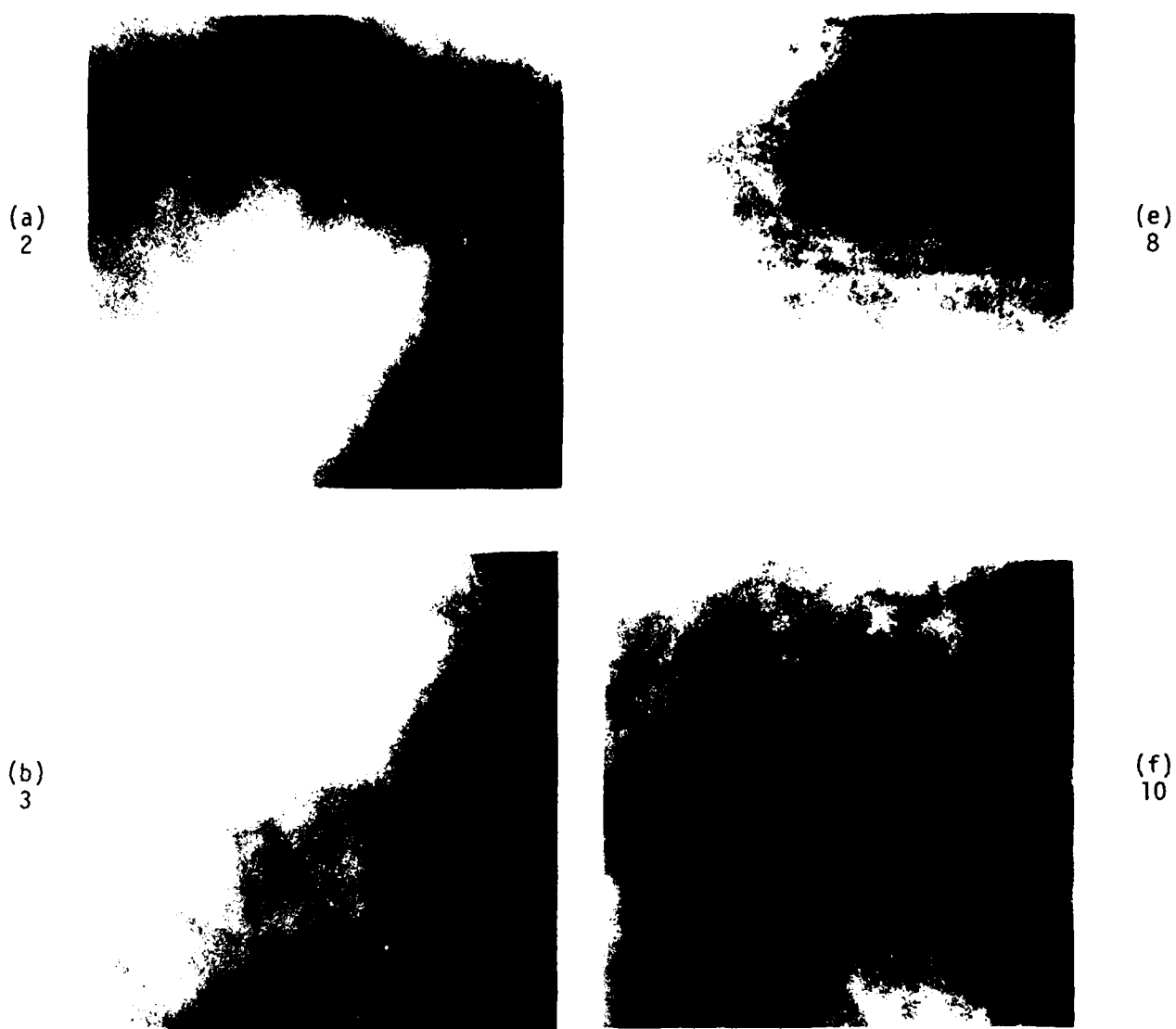
Figure 5. Channeling patterns corresponding to numbered grains in Figure 4.
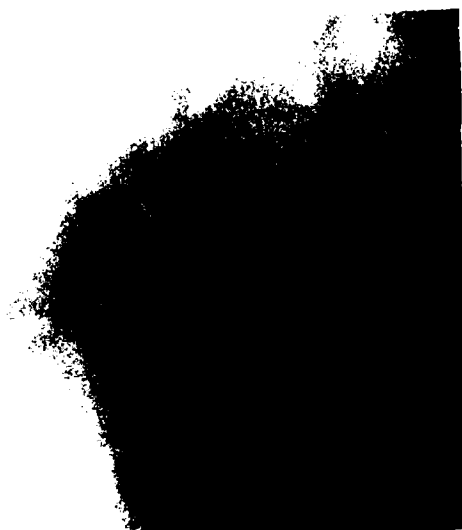
(c)
5

(g)
11

(d)
7

(h)
12

Figure 5 (Continued).   Channeling patterns corresponding to numbered
grains in Figure 4.

Study of Figure 5 produces an impression of generally poor electron channeling pattern contrast, with no obvious relationship between pattern clarity and the location of grains relative to the origin. Comparison of Fugure 5 with Figure 2 indicates that only grains 5 and 12 (Fig 3-c,h) yield patterns comparable to the undeformed state. In all other cases, the patterns are broadened, with some (Fig. 5-a, d, e) being barely recognizible as channeling patterns.

It is interesting to examine the possible relationship between channeling pattern quality and fracture mode. Grains 7 and 12, for example, have almost identical flat, striated fracture surfaces, yet channeling pattern from grain 12 is much sharper than that from grain 7 (Fig. 5-d, h). Near the origin (Figure 6), grains 1, 2, and 4 (Fig. 6-a, b) are extremely flat and smooth, suggestive of cleavage crack growth; nevertheless, the channeling patterns are non-existent for grains 1 and 4, and very diffuse for grain 2 (Fig. 5-b). On the other hand, grains 3 and 5 (Fig. 6-b, c) are composed of ledges, which might imply [11] enhanced plasticity. Nevertheless, while the channeling patterns produced by grain 3 (Fig. 5-b) are broad and diffuse, those obtained from grain 5 are very sharp, indicating a minimum of damage. From the foregoing, it seems that fractographic appearance does not offer a clear correlation with the degree of channeling pattern contrast.
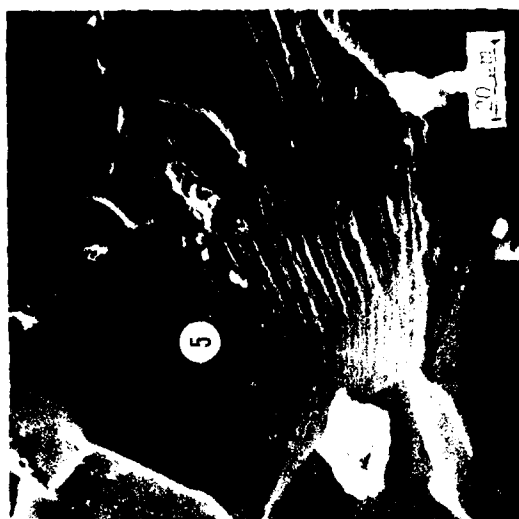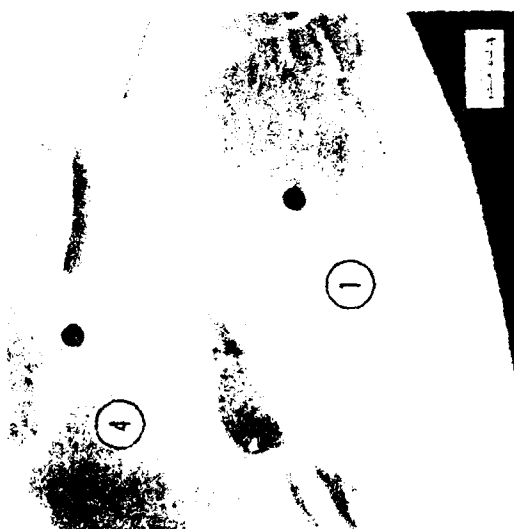
(a) Grains 1 and 4

(b) Grains 2 and 3

(c) Grain 5

Figure 6. High magnification view of fracture surface near origin.

DISCUSSION

1.   Interpretation of Results

Based on the loss of channeling pattern acuity within most of the grains traversed by a crack, it would appear that plasticity may be associated with crack extension. As of the present, it has not been possible to calibrate plastic strain in ceramics with channeling pattern change as has been done for metals [9], and the method of defect density assessment is not sufficiently far advanced [8] to assign either a strain value or a defect density to each of the fractured grains. Nevertheless, the line broadening is sufficient to cause one to suspect that a measurable increase in dislocation density should have been affected.

The fractured grains examined in this study exhibit a wide range of distortion, and although most of the channeling pattern lines in Figure 5 are too broad to permit accurate crystallographic orientation, they are sufficiently distinct to establish that the fracture planes possess a variety of orientations. Thus, it appears that crystallography may control the degree of channeling line distortion, hence by inference, the degree of local plasticity. On the other hand, the lack of correlation between channeling pattern quality and fractographic character suggests that the latter may not be a very reliable method by which to assess the nature of transcrystalline fracture in alumina. It is not obvious, for example, why one should expect lower ECP distortion from grain 5, Figure 4, than from the much smoother, more cleavage-like grain 1.

Several studies by other investigators tend to support the hypothesis that the observed ECP distortion should be interpreted in terms of crack tip plasticity. Guard and Romo [3], for example, used an X-ray microbeam technique to characterize crystalline deformation below transgranular tensile fracture surfaces of a similar polycrystalline alumina. A highly distorted layer, extending some 10 μm (∿ 1/2 grain) beneath the fracture surface, was detected. Since this zone was present for all crystallographic reflections, it was concluded that it must have been caused by multiple slip during passage of the crack.

In another program, Congleton, et al [1], obtained thin flakes produced during the passage of tensile cracks in Lucalox. These flakes were sufficiently thin to permit the transmission of electrons, and TEM photomicrographs of flakes generated during fracture at 600°C showed evidence of microtwinning and regions of high dislocation density. This temperature is far below that (∿ 1200°C) normally associated with dislocation motion in alumina. It should be noted, however, that whether the dislocations observed by Congleton, et al., were sessile, or glissile, was not established.

Finally, a study by Pollock and Hurley [12] of strain-rate-dependent fracture strength in sapphire filaments was interpreted in terms of dislocation-assisted crack growth. Evans, Wiederhorn, and Hockey [13] disagreed with this interpretation, and presented arguments for an alternative explanation, based on thermally activated crack growth. In the course of this rebuttal, however, the latter authors actually show

that the strain-rate dependence of the tensile strength σ_T correlates

very well with the strain rate dependence of the dislocation flow

stress σ_f. In particular, it was estimated that at room temperature,

$\dfrac{\Delta \log \dot{\epsilon}}{\Delta \log \sigma_f} \approx 24$, while $\dfrac{\log \dot{\epsilon}}{\log \sigma_T}$ was determined to be 28. (The argument

against a dislocation mechanism then reduces to one involving the stress

raising capacity of crack nucleating voids, and the relative density of

nearby pre-crack flaws).

On the other hand, there is at least one very strong piece of experi-

mental evidence which refutes altogether the idea of crack tip plasticity

in alumina. Wiederhorn, Hockey, and Roberts [2] have carried out an

exhaustive transmission electron study of arrested cracks at indentations

in sapphire and alumina. Cracks of various crystallographic orien-

tations were examined, both at their tips, and back along their flanks.

Below 400°C, no evidence of dislocations or microtwins was associated

with any portion of the crack trace. It was hypothesized [2] that

thermally activated crack growth probably was caused by one of at least

three other possibilities: (1) crack growth via stress-induced diffusion

of vacancies; (2) fracture via atomic bond fluctuations at the crack tip;

(3) rearrangement of atomic bonds during the fracture process.

The only apparent major difference between various sets of experi-

ments, aside from the techniques employed, seems to be that in the tests

leading to inferred crack tip plasticity, the cracks studied had been

accelerating, while in the indentation crack study by Wiederhorn, et al.

[2], the cracks were arrested. It really is not evident, however, how

this difference might account for the observed variance in interpretation.

If it is true that there is no plasticity associated with passage of the crack tip, then the electron channeling and X-ray line distortions <u>must</u> be explainable on the basis of some other physical process related to fracture. For example, should the thermal activation process involve vacancy diffusion, then perhaps the observed distortion is due to the presence of local strain fields produced by an excess vacancy population near the fracture surface. Alternatively, the distortion might originate in altered near surface atomic bonding, induced by passage of the crack. On the other hand, electron channeling should sample [8] crystalline regions lying far below such a hypothetical localized "disordered" region, such that the contribution of the "disordered" region to each channeling pattern is only a small fraction of the total. In this case, fairly high quality diffraction lines would be expected. Similarly, during the X-ray experiments of Guard and Romo [3], the "disordered" region would have been removed during sequential etching; yet, it persisted far ($\gtrsim 10$ μm) into the specimen.

To resolve this issue, it would be extremely helpful to combine some of the experiments which have been carried out to date. For example, it would be informative to use electron channeling to interrogate the fracture surface of a specimen broken at an indentation precrack. Study of the region within the precrack, and also outside of it, would correspond to analysis of both decelerating and accelerating cracks in the same specimen. Thin foils of each region for TEM study would provide a direct comparison between TEM and electron channeling. Such experiments are planned.

ACKNOWLEDGEMENTS

REFERENCES

1. J. Congleton, N. J. Petch, and S. A. Shiels, Phil. Mag. 19 (1969) 795.

2. S. M. Wiederhorn, B. J. Hockey, and D. E. Roberts, Phil. Mag. 28 (1973) 783.

3. R. W. Guard and P. C. Romo, J. Am. Cer. Soc. 48 (1965) 7.

4. J. Lankford, J. Mat. Sci. 13 (1978) 351.

5. J. Lankford, J. Mat. Sci. 12 (1977) 791.

6. J. Lankford and D. L. Davidson, The Science of Ceramic Machining and Surface Finishing II, NBS Special Publication 562, Ed. B. J. Hockey and R. W. Rice, U. S. Department of Commerce, Washington, D.C. (1979) 395.

7. J. Lankford and D. L. Davidson, J. Eng. Mat. Tech. 98 (1976) 17.

8. D. L. Davidson, "Assessment of Defect Magnitude by Changes in Selected Area Electron Channeling Patterns," SEM 1981 (in press).

9. D. L. Davidson and J. Lankford, J. Eng. Mat. Tech. 98 (1976) 24.

10. J. Lankford and D. L. Davidson, J. Mat. Sci. 14 (1979) 1669.

11. J. L. Henshall, D. J. Rowcliffe, and J. W. Edington, J. Am. Cer. Soc. 60 (1977) 373.

12. J. T. A. Pollock and G. F. Hurley, J. Mat. Sci. 8 (1973) 1595.

13. A. G. Evans, S. M. Wiederhorn, and B. J. Hockey, J. Mat. Sci. 9 (1974) 1367.

DATE

ILMED

-8